
HySCORE: Hydrogen Storage Characterization and Optimization Research Effort

Thomas Gennett (Primary Contact), Philip Parilla, Katherine Hurst, Madison Martinez; postdocs: Noemi Leick, Sarah Shulda, Jacob Tarver (NIST), Robert Bell, Mirjana Dimitrievska (NIST), Craig Brown (NIST)
National Renewable Energy Laboratory
15013 Denver West Parkway
Golden, CO 80401
Phone: (303) 384-6628
Email: thomas.gennett@nrel.gov

Jeffrey R. Long, Martin Head-Gordon
Lawrence Berkeley National Laboratory
1 Cyclotron Rd
Berkeley, CA 94720
Phone: (510) 642-0860
Email: jrlong@lbl.gov

Tom Autrey, Mark Bowden, Abhi Karkamkar, Bojana Ginovska, Iffat Nayyar; graduate students: Phuong Nguyen, Sunil Shrestha
Pacific Northwest National Laboratory
902 Battelle Blvd
Richland, WA 99354
Phone: 509-375-3792
Email: tom.autrey@pnnl.gov

DOE Manager: Jesse Adams
Phone: (720) 356-1421
Email: Jesse.Adams@ee.doe.gov

Project Start Date: October 1, 2015
Project End Date: Project continuation and direction determined annually by DOE

- Unravel complex phenomena, guide experimental work, and accelerate progress.
- Develop *in situ* infrared spectroscopy as a tool for characterizing emerging hydrogen storage materials that may allow for a driving range greater than 300 miles.
- Seek materials with the potential for meeting the DOE targets of reversible uptake.
- Validate new concepts for hydrogen storage mechanisms in adsorbents.
- Provide accurate computational modeling for hydrogen adsorbed in porous materials.
- Develop a series of advanced characterization tools that allows for rapid advancement and in-depth understanding of next-generation hydrogen storage materials.
- Develop a hydrogen storage material with a total materials-based capacity of >45 g/L above 150 K, that is possible with hydrogen overpressures <100 bar and reversible for multiple cycles.
- Optimize thermal management in hydrogen storage systems by the incorporation of unique phase-change materials.
- Demonstrate the importance of computational methods in developing and understanding of next-generation hydrogen storage materials.

Overall Objectives

- Advance the core competencies of the DOE Fuel Cell Technologies Office (FCTO) program as related to the characterization, evaluation, qualification, and validation of next-generation and current hydrogen storage materials.
- Benchmarking theory:
 - Couple theory with experiment to benchmark and validate the computational predictions (Hydrogen Materials Advanced Research Consortium [HyMARC] collaboration).

Fiscal Year (FY) 2018 Objectives

- Integrate the HySCORE and HyMARC programs to a cohesive, synergistic collaborative group.
- Develop and validate a cryo-PCT (pressure, composition, temperature) system for hydrogen sorption measurements from 40–303 K and up to 150 bar.
- Devise a methodology for the diffuse reflectance infrared Fourier transform spectroscopy (DRIFTS) measurements, allowing us to extract the thermodynamic parameters of hydrogen binding in complicated systems.

- Assist seedling projects with PCT, thermal conductivity, thermally programmed desorption (TPD), thermogravimetric analysis, and DRIFTS, and help them meet their go/no-go metrics.
- Develop international accepted protocol for determination of volumetric capacities.
- Validate samples for hydrogen storage capabilities as determined by DOE.
- Develop and characterize materials with validated coordinately unsaturated metal centers, and/or advanced hydrides and/or framework and/or templated materials within the hydrogen storage matrix that result in volumetric capacities in excess of 45 g/L, targeted enthalpies in the ideal range of 15–20 kJ/mol, acceptable gravimetric capacities, and the ability to deliver on-demand hydrogen at an appropriate rate and pressure for hydrogen fuel cell vehicles at temperatures from 150–225 K and initial overpressure <100 bar.
- Research and development of metal-organic framework (MOF) materials with high volumetric and gravimetric hydrogen capacities.

Technical Barriers

This project addresses the following technical barriers from the Hydrogen Storage section of the Fuel Cell Technologies Office Multi-Year Research, Development, and Demonstration Plan¹:

- (A) System weight and volume
- (B) System cost
- (E) Charging/discharging rates
- (O) Lack of understanding of hydrogen physisorption and chemisorption
- (P) Reproducibility of performance.

Technical Targets

This project is conducting validation studies of various framework materials, sorbents, hydrides, and model compounds. Concurrently, the team

also is developing new characterization tools for the rapid enhancement of materials development. Insights gained from these studies will be applied toward the design and synthesis of hydrogen storage materials that meet the following DOE onboard 2020 automotive hydrogen storage targets.

- 1.5 kWh/kg system (4.5 wt% hydrogen)
- 1.0 kWh/L system (0.030 kg hydrogen/L)
- Cost of \$10/kWh (\$333/kg H₂ stored)
- An onboard efficiency of 90% and minimum delivery pressure of 5 bar
- Total refuel time of 3–5 min.

FY 2018 Accomplishments

National Renewable Energy Laboratory (NREL)

- Installed and validated performance of the variable-temperature PCT apparatus (Performance Evaluation and Measurement Plan [PEMP] Milestone). NREL completed the aforementioned milestone for isosteric heat determination and, in the process, discovered several issues that need addressing to inform the interpretation of such determinations and to do so accurately and without bias.
- Determined the ability to utilize vibrational phonons to kinetically control the release of hydrogen from a series of C2N framework materials.
- Established/validated multiple samples from seedling projects, with two “go” decisions on projects moving forward.
- Established that in volumetric determination of hydrogen sorption, the major systematic errors lie in the determination of void volumes and packing densities—achieved through a 15-lab interlaboratory collaboration.
- Established a new collaborative partner, Michael Toney at SLAC National Accelerator Laboratory, and placed an NREL postdoc on-site at SLAC in August 2018.

¹ <https://www.energy.gov/eere/fuelcells/downloads/fuel-cell-technologies-office-multi-year-research-development-and-22>

- Added capability: Supercritical CO₂ Extraction for Purification of Porous Materials.
 - Many of the highly porous sorbents have suffered from solvents clogging pores. NREL installed a supercritical CO₂ extractor that assists in the removal of solvent molecules prior to any treatment (degassing) for TPD, Brunauer-Emmett-Teller, or PCT measurements.
 - The procedure still needs to be optimized for different materials and different solvents to ensure that the cleaning process successfully removes the impurities.
- Coordinated with Sandia National Laboratories and DOE to author and publish a perspective on the use of hydrogen storage sorbents for transportation applications.

Lawrence Berkeley National Laboratory (LBNL)

- Installed *in situ* infrared spectrometer and validated the performance of the instrument at 15–373 K and 0–100 bar.
 - Installed variable temperature capability on the DRIFTS instrument.
 - Validated the variable-temperature infrared (VTIR) method for determining

thermodynamics of adsorption by comparison with published materials.

- Extensively studied the thermodynamics of H₂ binding in Cu^I-MFU-4l using *in situ* DRIFTS.
- Targeted the synthesis of a room-temperature physisorption hydrogen storage material with a high density of unsaturated metal sites.
 - Synthesized a pyridinyl phenol-containing variant of UiO-67 and metalated with Cu(I) and Li(I).
 - Synthesized two new frameworks of the M₂(dotpdc) (MOF-374) structure type containing *N,N*-chelating groups for metalation.
 - Synthesized a new V(II) framework that binds hydrogen with an optimal adsorption enthalpy for ambient-temperature storage.
- Determined a computational protocol for binding energy computation and analysis, infrared spectra, and enthalpy-entropy relationship for sorbent materials.
- Benchmarked a dataset tailored for hydrogen storage to identify cheap, high-performance density functionals.

INTRODUCTION

NREL

This collaboration is predicated on a synergistic approach to further validate hydrogen storage concepts and develop the key core capabilities necessary for accurate evaluation of hydrogen storage materials capacity, kinetics, and sorption/desorption physio-chemical processes. The overall approach involves collaborative experimental and modeling efforts. We are validating concepts and utilizing core capabilities to rapidly define, model, synthesize, and characterize the appropriate materials necessary for achieving the vehicular hydrogen storage goals set forth by DOE. The approach is multifaceted to mitigate risk and ensure success as we bridge the gap between physisorption and chemisorption to provide the basis for a new generation of hydrogen storage materials technologies.

LBNL

Porous framework materials, such as MOFs, represent several possible paths forward toward a hydrogen storage adsorbent that can, at minimum, exceed the capabilities of current high-pressure onboard storage tanks and ultimately meet the system storage targets set by the DOE. However, the binding energies and volumetric capacities for hydrogen uptake are still not within the required range. Therefore, the critical objective with adsorbents is to design and synthesize porous framework materials replete with strong hydrogen binding sites that are suitable for the room-temperature hydrogen adsorption and desorption.

Our work to develop hydrogen storage adsorbent materials is performed in collaboration with NREL, Pacific Northwest National Laboratory (PNNL), and the National Institute of Standards and Technology (NIST). Key activities at LBNL include synthesis of frameworks that adsorb hydrogen with an enthalpy (isosteric heat of adsorption Q_{st}) in the optimal range of -15 to -25 kJ/mol, preparation of frameworks with open metal sites that adsorb more than two hydrogen molecules, and variable-temperature DRIFTS analysis to collect thermodynamic parameters for hydrogen adsorption, as well as benchmarking density functional theory functionals for hydrogen storage in MOFs.

PNNL

The Hydrogen Storage subprogram supports research and development of technologies to lower the cost of near-term physical storage options and longer-term material-based hydrogen storage approaches. The program conducts R&D of low-pressure, materials-based technologies and innovative approaches to increase storage potential and broaden the range of commercial applications for hydrogen. These advanced-materials activities focus on development of core capabilities designed to enable the development of novel materials with the potential to store hydrogen near room temperature, at low-to-moderate pressures, and at energy densities greater than either liquid or compressed hydrogen on a systems basis. Key activities include improving the energetics, temperature, and rates of hydrogen release. Advanced concepts include high-capacity metal hydrides, chemical hydrogen storage materials, and hydrogen sorbent materials, as well as novel material synthesis processes. The overarching goal of the FCTO Hydrogen Storage subprogram is to develop and demonstrate viable hydrogen storage technologies for transportation, stationary, portable power, and specialty vehicle applications (e.g., material handling equipment, airport ground support equipment), with a key goal of enabling >300-mile driving range across all light-duty vehicle platforms, without reducing vehicle performance or passenger cargo space.

APPROACH

NREL

Our approach in FY 2018 included efforts to develop state-of-the-art characterization techniques for hydrogen storage materials including advanced thermal conductivity, PCT, cyclotron X-ray techniques, and neutron-based spectroscopic techniques. Through theoretical-experimental iterations, we focused on addressing questions and validating recent concepts and mechanisms related to the materials-based hydrogen storage community including:

- How do multiple hydrogen molecules adsorb on an unsaturated metal center within a sorbent?
- Is it possible to enhance the kinetics of hydride formation with additives?
- Can we control the desorption temperature through the manipulation of dynamic materials?
- How can one alter/increase the hydrogen binding energies for physisorption in non-crystalline and crystalline sorbents?

Our team directly interacts with and supports the entire HyMARC core team, as well as the HyMARC seedling projects.

LBNL

To enhance hydrogen storage capacity, MOFs with a greater density of strong binding sites on the pore surface need to be developed. Our approach incorporates organic linkers with coordinating functionalities into framework materials, which will be used to append extra-framework cations to the pore wall. Taking advantage of the framework structure to immobilize these cations in the void volume of the material, low-coordinate metals capable of binding multiple H₂ molecules at each site were targeted. Our work in FY 2018 includes optimizing routes for metalation and activation to achieve a high density of metal cations bearing multiple coordination sites for H₂ binding. In parallel with synthetic efforts, *in situ* VTIR measurements are carried out to evaluate the thermodynamic properties of framework materials. Indeed, infrared spectroscopy is a powerful technique that can be used to gain site-specific adsorption information through the spectroscopic observation of vibrational modes associated with adsorbed hydrogen. In the theory work, we began benchmarking of density functionals for hydrogen storage in porous materials in order to identify inexpensive, high-performance density functionals.

PNNL

PNNL is developing advanced characterization capabilities to provide critical approaches to validate theories and test concepts proposed in the development of new details into the chemical and physical properties of hydrogen storage materials.

- Variable-pressure magic angle spinning (MAS) nuclear magnetic resonance (NMR): Variable-pressure (1–200 bar), variable temperature (298–473 K), *in situ* multi-nuclear solid state MAS NMR is being developed to identify key intermediates in the release and uptake of hydrogen in complex metal hydrides to validate claims that additives control selectivity and enhance reversibility.
- Low-temperature solid-state NMR: Low temperature (to 5 K) solid-state ¹H NMR is being developed to measure the enthalpy of adsorption of H₂ to high-surface-area storage materials and provide the ability to validate the concept that more than one H₂ molecule can bind to a metal site on a high surface amorphous material.
- Variable-pressure liquid NMR: Variable-pressure (1–100 bar), variable-temperature (250–350 K), multi-nuclear liquid NMR is available to measure key intermediates, kinetics, and thermodynamics of hydrogen release and uptake in liquid carriers.
- Variable-pressure calorimetry: Variable-pressure (1–20 bar), variable-temperature (298–353 K) reaction calorimetry is being developed to measure kinetics and enthalpies of H₂ uptake in liquid and solid stores to benchmark and validate computational predictions of binding enthalpies in liquid carriers.

In FY 2018 our work focused on efforts to develop advanced characterization techniques for hydrogen storage materials with special emphasis on calorimetry and *in situ* NMR spectroscopy. We worked toward developing new capabilities to validate theories and novel concepts proposed by the research community; a parallel research effort on materials evaluation complements the characterization capability development. Through a

theoretical/experimental interaction, our research focus was (1) determination of the thermodynamics of H₂ uptake and release from liquid carriers (i.e., phenol, formic acid) as part of a collaboration with Dr. Karsten Mueller (Erlangen University) and Dr. Teng He (DICP), (2) binding energies of H₂ to B-doped carbon when B is located on the edge of the coronene, and (3) thermodynamics of the recycling of solvent-free Mg(B₃H₈)₂ and Mg(BH₄)₂ as part of a collaboration with Prof. Hans Hagemann (University of Geneva). In addition, we were able to assist a number of HyMARC seedling projects in their characterization efforts using NMR, X-ray diffraction, and transmission electron microscopy spectroscopies.

RESULTS

NREL

This report describes the major accomplishment of meeting the DOE-PEMP milestone using the variable-temperature PCT apparatus at NREL. The sorbent material chosen was a commercially available activated carbon known as Norit ROW 0.8, which is in a pelletized form and has been used by NREL as a standard material for testing PCT instrumentation and for interlaboratory comparisons of hydrogen capacity [1–2]. After degassing, the final mass for the sample was 1.404 g, which provided excellent signal to noise even at the higher temperatures. A series of six different temperatures were chosen at which to measure the isotherms up to pressures of ~100 bar. All isotherms consist of at least one full cycle (adsorption and desorption), and several had more. The six temperatures were grouped into three pairs so that different methods of determining the isosteric heats (Q_{st}) could be tested; the three pairs are (77 K, 87 K), (100 K, 110 K), and (273 K, 303 K). The resulting isotherms are shown in Figure 1.

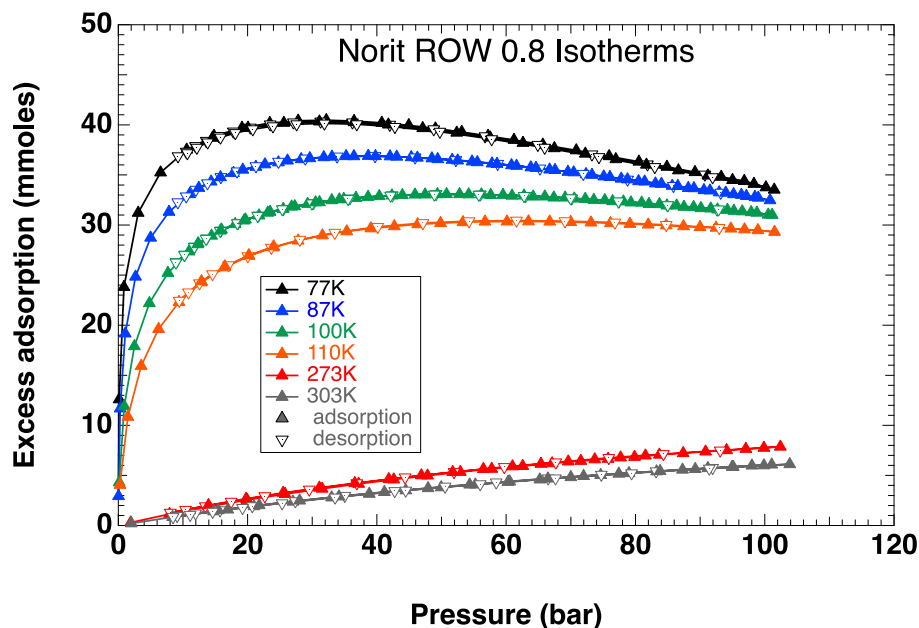


Figure 1. The isotherms obtained and used for the isosteric heat calculations on the new variable-temperature PCT apparatus

Isosteric heats can be calculated in various ways. The main definition often found in the literature is:

$$q_{st} = RT^2 \left(\frac{\partial \ln(P)}{\partial T} \right)_n = -R \left(\frac{\partial \ln(P)}{\partial \left(\frac{1}{T} \right)} \right)_n \quad (1)$$

Where q_{st} is the isosteric heat, R is the universal gas constant, T is the temperature, and P is the pressure. The n subscript indicates the adsorbed moles is held constant. A discretized version for two isotherms taken at similar temperatures, T_1 and T_2 , is:

$$q_{st} = RT_1T_2 \left(\frac{\ln(P_2/P_1)}{T_2 - T_1} \right)_n \quad (2)$$

Where again the n indicates that the pressures are at the same mole loading. Probably the most robust technique is to plot $\ln(P)$ versus $1/T$ for several temperatures to check for linearity and to measure the slope of the line, which is equal to $-q_{st}/R$ [3–4].

Because any isosteric calculations must be performed at equal mole loading, keeping the isotherms in moles is desirable. (By convention, with the PCTPro reporting standards, moles are reported as *atomic* hydrogen, not *molecular* hydrogen.) For the 77 K data, this is maximum near 30 bar and corresponds to approximately 2.82 wt% and is consistent with previous NREL measurements and the recently completed interlaboratory comparison. Also, because of the requirement for equal mole loading for the calculation, a robust method is needed to interpolate between the actual data points of the isotherm. For the very steep rise at low pressures and low temperatures, this is non-trivial. A linear interpolation method was tried and proved to be inadequately accurate. Instead, the data was fit with a Sips isotherm (Equation 3; also known as a Langmuir-Freundlich) [5–6].

$$n_{ad} = \frac{n_0(bP)^{\frac{1}{m}}}{1 + (bP)^{\frac{1}{m}}} \quad (3)$$

Where n_{ad} is the amount adsorbed as a function of pressure, P , n_0 is the saturation adsorption amount, m is the exponent factor, and b is a parameter that depends on the temperature and other factors corresponding to the physical processes of the adsorption sites. Because this is a strictly monotonically increasing function, only the initial part of isotherms was fit for those isotherms that were not monotonically increasing (i.e., the low-temperature data). An example of that fit is given in Figure 2 for the 110 K data.

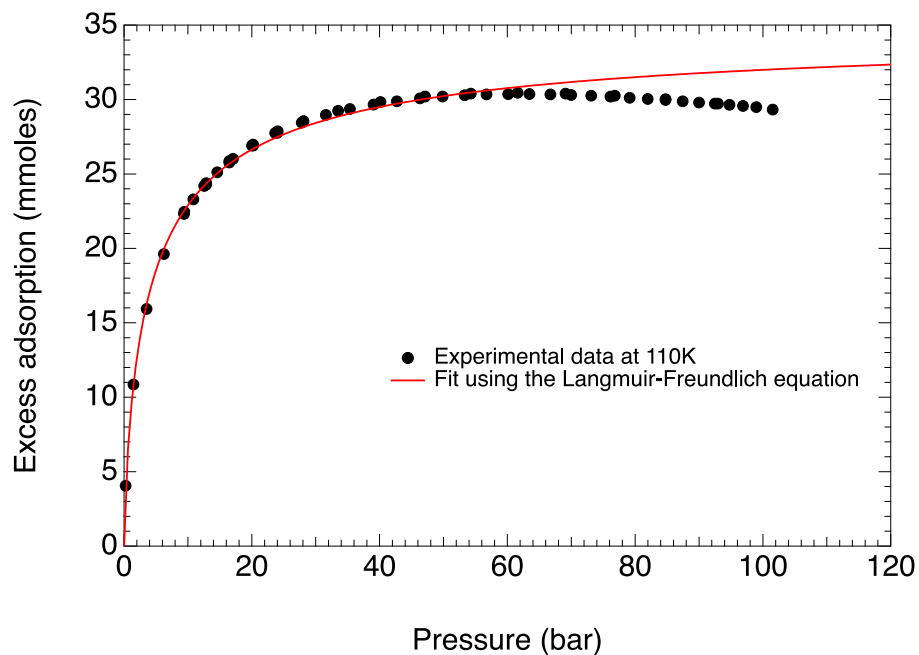


Figure 2. An example of how the isotherms were fit using the Langmuir-Freundlich isotherm function model

These fits can be inverted (i.e., solved for the pressure, P), which then becomes pressure as a function of moles adsorbed at a given temperature.

$$P = \frac{1}{b} \left(\frac{n}{n_0 - n} \right)^m \quad (4)$$

Using these inverted fit functions, the $\ln(P)$ versus $1/T$ plot at various loadings can then be made and linear fits can be performed to get the slopes yielding the isosteric heats. Figure 3 shows the result of this plot and fits for a subset of the data.

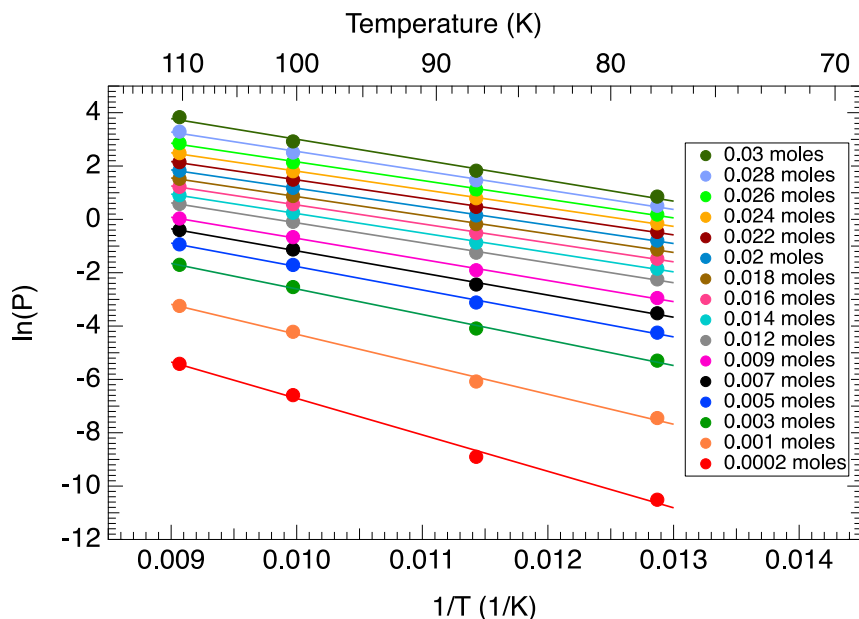


Figure 3. An example of how the isosteric heats at various mole loadings were determined from the slope of lines fitted with the $\ln(P)$ versus $1/T$ data

It can be seen from the data that a linear fit is a reasonable model at these low temperatures. While most of the linear fits are roughly parallel, and thus indicate similar Q_{st} , at the lower mole loadings the slopes are increasingly negative and indicate higher Q_{st} . This is all summarized in Figure 4, which shows the Q_{st} derived from the linear fits as a function of mole loadings again from the low-temperature data. There is a relatively constant region near 6 kJ/mole, and this agrees reasonably well with a measurement on Norit ROW 0.8 that found an average of 5 kJ/mole over surface coverages between 36% to 82% [3]. For the NREL data at low-mole loadings, the Q_{st} approaches 11 kJ/mole. There are two possible reasons for this. *First*, in the low-mole region, the isotherms at low temperature are very steep and difficult to model, and small errors in this modeling can lead to large errors in the calculation. In fact, the aforementioned literature reference deliberately avoided reporting their data in this region precisely because of this issue [3]. What is needed to get accurate low-mole estimates of the Q_{st} is to obtain a larger number of data points in the fast-rising part of the isotherm. *Second*, it is not unreasonable to expect that, for a heterogeneous adsorption surface, the stronger adsorption sites will be occupied first and so could truly represent the higher energy sites. There is also an upturn in calculated energy at high loadings. This is a well-known effect that results from the fact that the measured isotherms actually are excess capacity isotherms, not the absolute isotherms that are required for the true isosteric determination [4, 7]. Because only excess isotherms can be measured in the real world, additional modeling is needed to attempt to compensate for this; this modeling is outside the scope of this report.

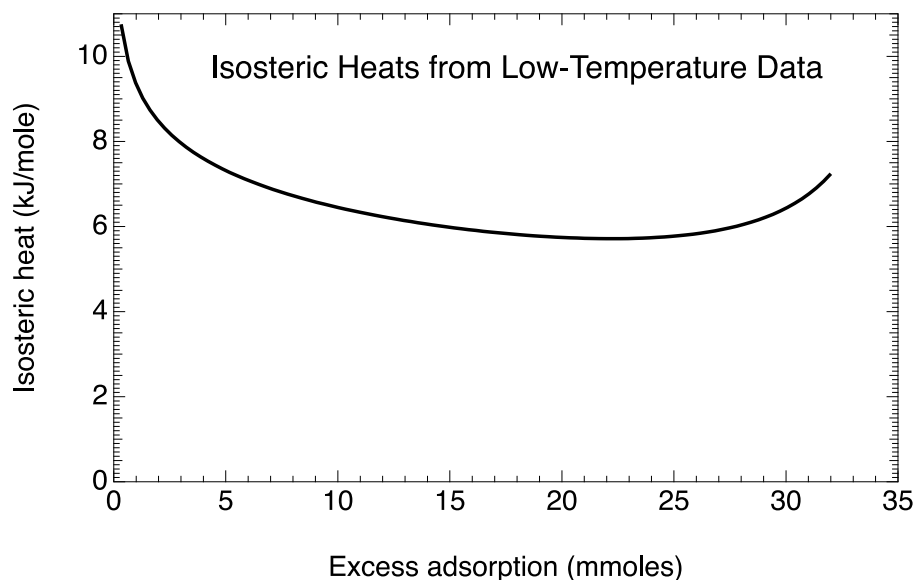


Figure 4. The isosteric data versus mole loadings from all the fitted lines of the $\ln(P)$ versus $1/T$ data. See text for detailed discussion.

To briefly summarize, NREL has successfully completed the milestone to measure the isosteric heats and has achieved good agreement with a previous measurement from the literature. During the effort to complete this milestone, NREL has discovered several issues in both measuring the data and analyzing the data, which is work continuing into FY 2019.

NIST (as part of NREL)

Structural and Dynamical Trends in the Alkali-Metal Silanides ($MSiH_3$, $M = K, Rb, Cs$) and the Potential Effect on their Hydrogen Storage Properties

We worked on elucidating the dynamical details of both the α - and β -phases of alkali-metal silanides ($MSiH_3$, $M = K, Rb, Cs$) to investigate their potential use for hydrogen storage applications. Characterization of the structures and possible SiH_3^- reorientational dynamics of these compounds was performed using various neutron scattering techniques, including neutron powder diffraction, neutron vibrational spectroscopy, neutron scattering fixed window scans, and quasielastic neutron scattering measurements (QENS). The results show that the phase transition leads to dynamical changes corresponding to the onset of rapid reorientational motions of the pyramidal SiH_3^- ions. An unusual nature of the anion dynamical transformation was observed upon transitioning between the α -phase and β -phase. Based on the dynamical measurements and calculations from QENS spectra, a phase diagram was constructed for $CsSiH_3$ presenting an evolution of different phases with the temperature. Besides being of considerable fundamental interest, these results provide better understanding of the nature of the SiH_3^- orientational mobility in the disordered and ordered phases, as well as give more detailed insights into the origin of these materials' favorable hydrogen storage properties. This work was submitted and recently published in: M. Dimitrievska, "Tracking the Progression of Anion Reorientational Behavior between α -phase and β -phase Alkali-Metal Silanides by Quasielastic Neutron Scattering," *J. Phys. Chem. C* 122, no. 42 (2018): 23985–23997.

LBNL

Materials Synthesis

Synthetic efforts at LBNL focused on the continued research into and synthesis of compounds that have the potential to bind multiple hydrogen molecules to a single metal center. One of the typical examples is synthesis of a pyridinyl phenol-containing variant of UiO-67, followed by the metalation with various metal cations.

Specifically, a derivative of UiO-67 [$\text{Zr}_6\text{O}_4(\text{OH})_4(\text{PhOHpydc})_6$; $\text{H}_2\text{PhOHpydc} = 6$ --(4-carboxy-2-hydroxyphenyl)nicotinic acid] that contains free pyridine and phenol groups on the linker capable of acting as a chelating binding site was successfully synthesized (Figure 5). The material shows high crystallinity after desolvation of the framework with a high Langmuir surface area of $2,750 \text{ m}^2/\text{g}$. A variety of solvents containing mesitylcopper(I) or *n*-butyllithium were utilized for framework metalation. From inductively coupled plasma–optical emission spectrometry analysis, maximum Cu and Li loadings are estimated to be 0.1 and 4.2 per formula unit, respectively. Although the Cu-loaded framework showed a slight increase in low-pressure hydrogen uptake, Li samples showed decreased H_2 uptakes compared to the pristine framework, which is likely due to incomplete desolvation of the metalated framework even after thermal treatment *in vacuo*. Investigation of the optimal activation condition to prepare metalated frameworks with reasonable porosity is now in progress.

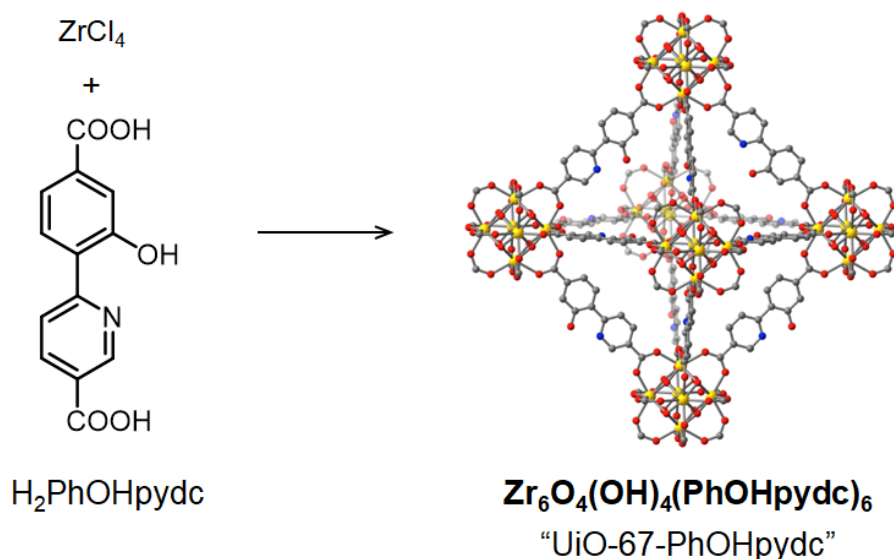


Figure 5. Synthesis and structure of UiO-67-PhOHpydc. Atom colors: C, gray; O, red; N, blue; Zr yellow; all hydrogen atoms are omitted to clarify.

Correlation Between Adsorption Enthalpy and Entropy

A target of -22 to -25 kJ/mol for the H_2 binding enthalpies has often been cited as optimal for physisorption materials [8]. However, this target assumes a strict enthalpy-entropy relation in order to arrive at the final ΔG° of adsorption. Theoretically, all enthalpy-entropy combinations giving rise to the same ΔG° will yield the same usable capacity under a set of storage conditions. In other words, synthesizing a material with a smaller $-\Delta H^\circ$ and a smaller $-\Delta S^\circ$ for the same ΔG° will lead to easier heat management at no cost to capacity. It is therefore imperative that ΔS° is considered when assessing materials alongside other thermodynamic parameters, and steps should be undertaken to understand and rationally tune ΔS° in physisorption materials. In FY 2018, Cu^{I} -MFU-4l [$\text{Cu}_2\text{Zn}_3\text{Cl}_2(\text{btdd})_3$] [9] was chosen to study the correlation between adsorption enthalpy and entropy. Measurement of VTIR spectra of the framework Cu^{I} -MFU-4l under H_2 and D_2 has allowed extraction of thermodynamic parameters of H_2 binding (Figure 6). It is remarkable that while the ΔH° of adsorption is around twice that of $\text{Ni}_2(m\text{-dobdc})$, the ΔS° is lower (Table 1). This breaks the trend of enthalpy-entropy correlations observed in most physisorption materials [10], due to the unique back-bonding interaction observed in this framework between Cu^+ and H_2 , similar to those in Kubas-type molecular complexes (Figure 7).

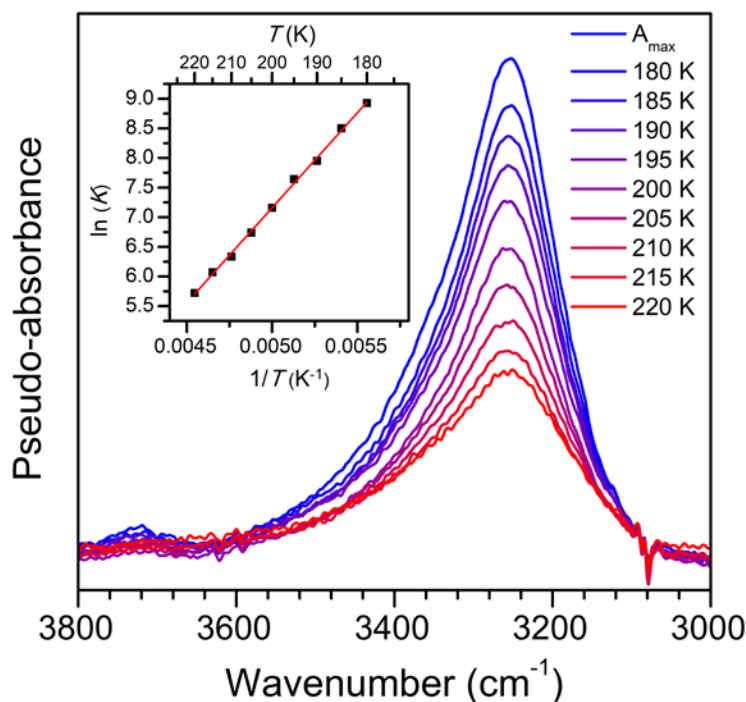


Figure 6. VTIR spectroscopy of H₂ adsorbed in Cu^I-MFU-4l. Spectra were generated by subtraction from corresponding D₂ dosed samples. Van't Hoff analysis yields a ΔH° of -26.7 kJ/mol and a ΔS° of -74 J/mol K. Cf. Ni₂(*m*-dobdc) $\Delta H^\circ = -13.6$ kJ/mol, $\Delta S^\circ = -85$ J/mol K.

Table 1. Summary of Metal Ion, Low-Pressure Excess Hydrogen Uptake, Initial Q_{st} Data, and Adsorption Enthalpy and Entropy Estimated from DRIFTS for Framework Materials Containing Open Metal Sites

MOF	Metal ion	H ₂ uptake at 77 K, 1 bar (mmol/g)	Q_{st} from isotherms (kJ/mol)	ΔH° from DRIFTS (kJ/mol)	ΔS° from DRIFTS (J/mol K)
Ni ₂ (<i>m</i> -dobdc)	Ni ²⁺	11.1	-12.3	-13.6	-85
V-MOF	V ²⁺	9.2	-21.0	-21.0	-84
Cu ^I -MFU-4l	Cu ⁺	8.1	-26.7	-33.6	-74

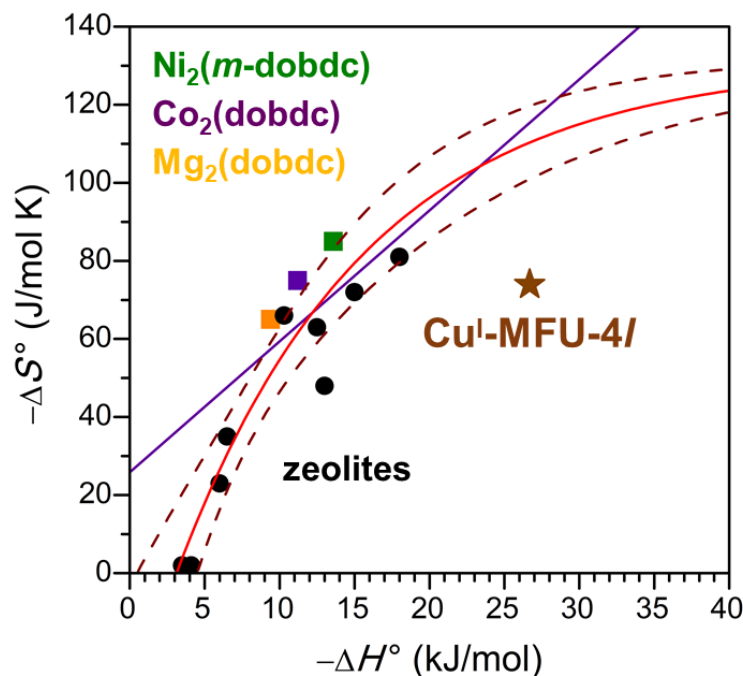


Figure 7. Thermodynamic parameters of H₂ adsorption in various sorbents. The approximate fit of enthalpy-entropy correlation for zeolites and M₂(dobdc) variants (red, 95% confidence intervals given by dark red dashed line) and optimal combinations of ΔH° and ΔS° for adsorption at 100 bar and desorption at 5 bar at 298 K (purple). Cu^I-MFU-4l represents a new class of physisorptive hydrogen adsorbents due to its unique mechanism of adsorption.

Electronic Structure Computations on Sorbents

For sorbent materials Cu^I-MFU-4l and V-MOF we have put in place a computational protocol to determine first the binding energy for small molecule adsorption, and we found significant covalent (chemisorptive) character in hydrogen binding. Infrared spectra were computed to corroborate DRIFTS measurements both in terms of spectral frequencies and to validate enthalpy/entropy relationships for the hydrogen binding event in sorbent materials. The substantial expertise in energy decomposition analysis has allowed us to study quantitatively the arrested oxidative addition of hydrogen to sorbents Cu^I-MFU-4l and V-MOF, which keeps binding enthalpy in the range (20–30 kJ/mol) ideal for hydrogen storage. Possible extensions to this protocol involve incorporating periodic corrections to electronic structure, and development of sorbent-specific force-fields.

Benchmarking Density Functionals for Hydrogen Storage

We began to compile a database for benchmarking the performance of density functional binding energies of hydrogen to a binding motif against high-quality reference data. The database currently consists of metal ions, salts, and organic linkers, which serve to mimic the environment of hydrogen binding in porous sorbent frameworks like MOFs. The benchmark data was generated using coupled cluster theory extrapolated to the complete basis set limit. Around 50 density functionals were studied and their errors were characterized in terms of basis set and density functional theory quadrature grid. While the density functional ω B97M-V provides the least root mean square error (RMSE) of 1.5 kJ/mol, we recommend the significantly cheaper B97-D3(BJ), which provides a slightly increased RMSE of 1.85 kJ/mol.

PNNL

Determination of the Thermodynamics of Hydrogen Uptake and Release from Liquid Carriers (i.e., phenol, formic acid)

Hydrogen storage in formic acid: a comparison of process options. Formic acid (53 g H₂/liter) is a promising liquid storage and delivery option for hydrogen for fuel cell power applications. In this work we compare and evaluate several process options using formic acid for energy storage. Each process requires different steps, which contribute to the overall energy demand. The first step (i.e. production of formic acid) is thermodynamically unfavorable. However, the energy demand can be reduced if a formate salt is produced via a bicarbonate route instead of forming the free acid from hydrogen and carbon dioxide. This *bicarbonate/formate* approach also turns out to be comparatively more efficient in terms of hydrogen release than the formic acid route. Even though less energy efficient, catalytic decomposition of formic acid has the advantage of reaching higher volumetric power densities during hydrogen release. Efficiencies of all process options involve aqueous media and are dependent on concentration. Heating water leads to additional energy demand for hydrogen release and thus lowers the overall efficiency. Separation and purification of hydrogen contributes a minor impact to the overall energy demand. However, its effect on efficiency is not negligible. Other process options like thermal decomposition of formic acid or direct formic acid fuel cells thus far do not appear competitive. For further details, please see *Energy & Fuels* (2017), DOI:10.1021/acs.energyfuels.7b02997.

Releasing hydrogen at high pressures from ambient condition carriers: aspects for the hydrogen delivery to fueling stations. Hydrogen fueling stations require multiple stages of compression to achieve the ca. 875 bar needed to refuel hydrogen fuel cell electric vehicles to 700 bar. The physical compression equipment constitutes a large share of the total investment cost of hydrogen fueling stations. Hydrogen carriers (i.e., materials that carry either physisorbed or chemisorbed H₂) provide an opportunity to simplify hydrogen delivery because they can transport higher densities of hydrogen to the fueling station at lower pressures. We introduce the term liquid phase hydrogen carriers (LPHCs) to be inclusive of liquid carriers that may not fall under purely organic (i.e., carbon based). Some LPHCs are defined by thermodynamic properties that allow hydrogen release at elevated pressure, thus providing an opportunity to reduce the number of compressors at the fueling station. This study compares a series of LPHCs and evaluates the approach of using aqueous solutions of formic acid as an alternate approach to deliver high volumetric densities of hydrogen to fueling stations and provide a first step of compression. Formic acid can be decomposed in a reactor to hydrogen and carbon dioxide at moderate temperatures and high pressure in the presence of a suitable catalyst. While hydrogen release from most liquid carriers will provide hydrogen slightly above ambient pressure at high temperatures, hydrogen release from the decomposition of formic acid will provide hydrogen at pressures of several hundred bar. A challenge of formic acid is that the high-pressure hydrogen is accompanied by an equivalent of carbon dioxide and thus requires subsequent separation and purification operations. Nevertheless, formic acid has the advantage of being liquid, which simplifies its handling and provides a continuous supply to a release unit. Furthermore, the energy demand for hydrogen release from formic acid is lower than for most alternative hydrogen carrier materials.

Thermodynamic modification of phenol-cyclohexanol couple (ca. 6 wt%, 57 g/liter). Addition or substitution of electron-rich heteroatoms (e.g., N) for C in cycloalkanes and arenes has been shown to favorably reduce the enthalpy difference between the hydrogenated and dehydrogenated hydrogen carrier with N-ethyl carbazole as a well-studied example. Clot, Eisenstein, and Crabtree published a computational study that provided the thermodynamic parameters (ΔH , ΔS and ΔG) for H₂ release from a series of N-containing arenes. They suggested that the addition of an electron-rich N may destabilize the cycloalkane, thus reducing the reaction enthalpy for H₂ release. Teng He in Ping Chen's group at DICP has been interested in modifying the thermodynamics of hydrogen storage material by substituting an H atom with an alkaline metal atom in compounds such as phenol and aniline. Figure 8 shows the calorimetric traces for heat of hydrogenation of (a) sodium phenoxide and (b) phenol respectively to cyclohexanol in water. ΔH for hydrogenation of sodium phenoxide was measured to be -182 kJ/mol (ΔH_{exp} 60.6 kJ/mol H₂ and ΔH_{calc} 60.9 kJ/mol H₂) while ΔH for

phenol was -206 kJ/mol (ΔH_{exp} 68.7 kJ/mol H_2 and ΔH_{calc} 64.5 kJ/mol H_2). The hypothesis was that the addition of an electronegative O onto the arene would provide an electron donating group comparable to N substitution. Furthermore, substitution of an Na for the H on the HO group could increase the electron density on the carbon framework further and decrease the enthalpy of H_2 release even further.

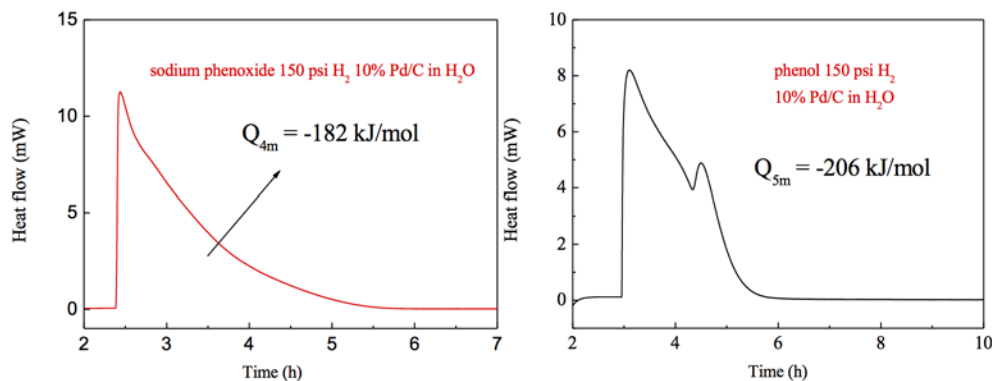


Figure 8. Calorimetric traces for heat of hydrogenation of (a) sodium phenoxide and (b) phenol respectively to cyclohexanol in water

In a related paper, Jessop and coworkers argued that there is a linear correlation between the Hammett σ (para) parameter and the enthalpy for H_2 release for a series of substituted N-substituted arenes. The more negative the Hammett σ (para) parameter, the lower the enthalpy for H_2 release. We used this hypothesis as a starting point to make predictions about the properties of phenol versus phenoxide as LPHCs in aqueous media. The results are promising and summarized below.

Binding energies of H_2 to B-doped carbon when B is located on the edge of the coronene. In addition to the previously reported binding energies of H_2 to B- and N-doped coronene model, where the doping was introduced in the central ring of the model system, we also explored possibilities of H_2 binding in cases where B is introduced at the edge (Figure 9).

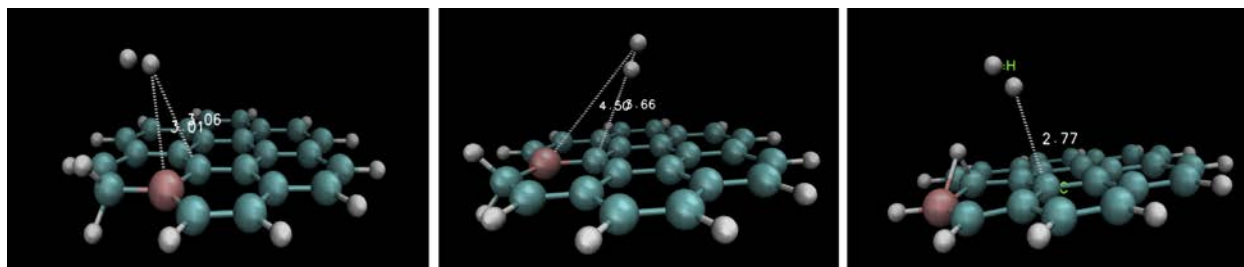


Figure 9. Image that illustrates H_2 binding in cases where B is introduced at the edge sites

As before, we used dispersion-corrected density functional theory (B3LYP+D3) level of theory, with 6-311G** basis set, using the NWChem computational package. All calculations were done in gas phase. We found that there is no improvement of the binding energy for the three different optimized stable structures, where the binding energies are in the range of 5.3 to 6.4 kJ/mol. Interestingly, when a single B atom is doped at the edge, where it is not H-terminated, the binding energy is lower than the binding of H_2 to undoped coronene, when the H_2 atom is in the vicinity of the B defect, but it is slightly stronger than coronene, when the interaction is predominantly with the carbon atoms in the center. Table 2 summarizes the binding energy of terminal B-doped coronene in comparison with previous values calculated for B inside central ring. When the B atom is H-terminated, it interacts with the H-terminal atoms on the neighboring carbon, forming an H-

bridged structure. In this case, the largest distortion from planarity is observed, and slightly enhanced binding energy.

Table 2. Binding Energies for Terminal B-Doped Coronene Compared with Previous Values Calculated for B Inside Central Ring

New values are displaced in bold italics and show no enhancement compared to non-terminal B-doped structures

System	Nomenclature	Binding Energy (kJ/mol H ₂)
C ₂₄ H ₁₂	C	6.2
B C ₂₃ H ₁₃	B	7.6
B C ₂₃ H ₁₃	<i>Bterm 1-1</i>	5.3
B C ₂₃ H ₁₃	<i>Bterm 1-2</i>	6.4
B C ₂₃ H ₁₃	<i>Bterm 2</i>	6.8
N C ₂₃ H ₁₃	N	6.7
B ₂ C ₂₂ H ₁₂	BB ortho	6.6
	BB meta	5.9
	BB para	5.6
B ₂ C ₂₂ H ₁₂	BN ortho	6.8
	BN meta	7.4
	BN para	6.9
B ₃ N ₃ C ₁₆ H ₁₂	BN cyclic	5.5

Thermodynamics of the recycling of solvent-free Mg(B₃H₈)₂ and Mg(BH₄)₂. Given the experimental challenge to make solvent-free Mg(B₃H₈)₂, we proceeded to perform experiments with the tetrahydrofuran (THF) adduct in collaboration with the University of Hawaii. We found that the THF adduct could be “reduced” to regenerate the corresponding Mg(BH₄)₂—a promising result that suggests calorimetry experiments could provide insight into the thermodynamics. We reported the result in previous quarterlies that provided an estimate of 70(10) kJ/mol H₂ for the difference between the THF adduct of B₃H₈ and the corresponding BH₄. This value was “high,” but far below the computational result suggesting 150 kJ/mol (for the solvent-free reaction). The result suggested that THF substantially stabilized the B₃H₈ intermediate, or the calculations were highly inaccurate, a troubling result.

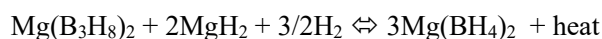
We considered two further options to help resolve the discrepancy. The calculations were performed on a “calculated” structure as no experimental structural insight is available for the Mg triborane—but an offset of 80 kJ/mol H₂ is unsatisfactory. Alternatively, the THF (i.e., a Lewis base) provided substantial stabilization compared to the solvent-free polyhedral boranes.

The results from the calorimetry experiments were not unambiguous. We were able to determine a lower limit for the hydrogenation reaction of -100 kJ/mol H₂. Notably this is greater than the hydrogenation of the THF adduct we reported previously, ca. -70 kJ/mol of H₂, but still far lower than the enthalpy predicted by theory, ca. -150 kJ/mol. We were able to provide a lower limit due to the observation that the solvent-free Mg(B₃H₈)₂ compound melts at ~80°C. In the presence of MgH₂ and H₂, the major product is the expected Mg(BH₄)₂. In the absence of MgH₂ and H₂, the major product is the closoborane, B₁₂H₁₂. We can only assign a lower limit given that the melting should generate an endotherm that reduces the magnitude of the exothermic for hydrogenation. However, several key takeaways were obtained:

- The solvent-free Mg(B₃H₈)₂ melts at a lower temperature than the THF adduct.
- The solvent-free Mg(B₃H₈)₂ decomposes upon melting whereas the THF adduct is meta-stable (i.e., it decomposes at a slightly higher temperature).
- The solvent-free Mg(B₃H₈)₂ decomposes to B₁₂H₁₂ and H₂ upon melting.

- The intermediates formed from decomposition of solvent-free $\text{Mg}(\text{B}_3\text{H}_8)_2$ can be trapped by the presence of MgH_2 and H_2 to form >95% corresponding BH_4^- , determined by *in situ* solid-state ^{11}B NMR and *ex situ* ^{11}B solution-phase NMR.
- The solvent-free $\text{Mg}(\text{B}_3\text{H}_8)_2$ reduction to $\text{Mg}(\text{BH}_4)_2$ is exothermic, ca. <-100 kJ/mol H_2 . This is more exothermic than reduction of the THF adduct, ca. -70 kJ/mol H_2 .

Figure 10 shows the *in situ* solid-state ^{11}B NMR comparing before and after heating solvent-free B_3H_8 to 100°C . The top panel shows $\text{Mg}(\text{B}_3\text{H}_8)_2$ neat resulting in formation of $\text{B}_{12}\text{H}_{12}$ and BH_4^- . The bottom panel is B_3H_8 decomposition in the presence of MgH_2 and H_2 , showing conversion of a broad B_3H_8 peak at -33 ppm to a sharp peak at -40 ppm, the BH_4^- . The middle panel compares decomposition of B_3H_8 in the presence of MgH_2 and no H_2 (red line) to decomposition with H_2 .



The enthalpy of hydrogenation is determined from the heat measured by calorimetry. Changing the sign provides the heat for making $\text{Mg}(\text{B}_3\text{H}_8)_2$ from $\text{Mg}(\text{BH}_4)_2$. An experimental value of 100 kJ/mol H_2 to compare with theory, ca. 150 kJ/mol H_2 . Experimental conditions use an excess of MgH_2 (4 equivalents) and H_2 (10 bar) to trap intermediates and push the reaction to BH_4^- .

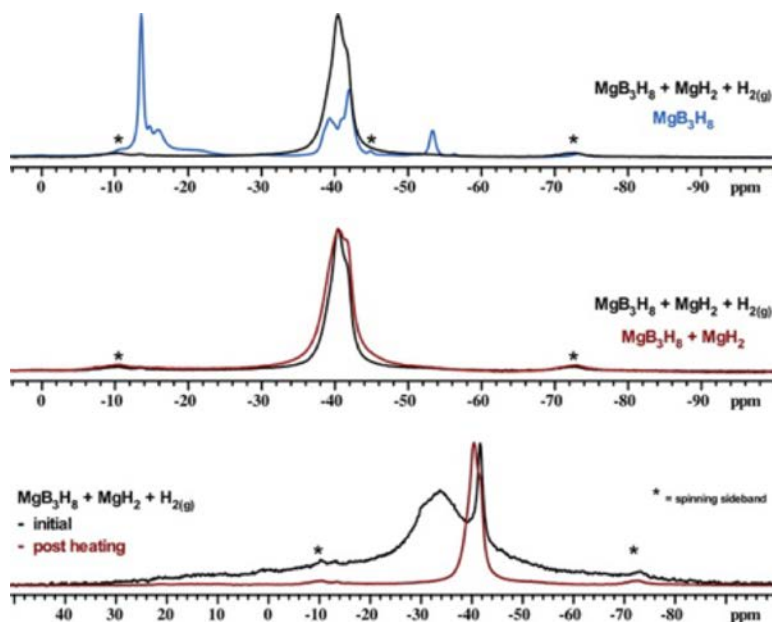


Figure 10. *In situ* solid-state ^{11}B NMR spectra comparing before and after heating solvent-free B_3H_8 to 100°C

CONCLUSIONS AND UPCOMING ACTIVITIES

NREL

In FY 2018 we made a considerable number of no-go decisions on various carbon-based sorbent materials, including B-doped carbon systems, biomass pyrolyzed products, and C2N materials with considerable purification issues. We also showed considerable success, as the diameter of a pore approaches the kinetic diameter of hydrogen, vibrational phonon modes, and not van der Waals interactions, can dominate the sorption kinetics and temperature of the sorption/desorption cycle. With respect to characterization the new variable-temperature PCT and thermal conductivity apparatus have proven to be a boon for the understanding of materials sorption processes.

In FY 2019 we have a considerable number of new initiatives that include sorbents, hydrides, and new characterization techniques for transportation, carriers, and long-term storage applications. Furthermore, the new variable-temperature PCT has also put forth a limitation of current theory/models toward the characterization of isosteric heats of adsorption. This is especially true as the sorption processes approach room temperature and the excess and absolute capacity of materials diverge. Specifically, the following are issues that need to be examined more carefully.

Experimental:

- Adequate isotherm data collection (especially steep part of curve)
- Sensitivity analysis to calibration errors (similar to excess versus absolute).

Analysis:

- Very accurate fitting/interpolation of data is required.
- Excess versus absolute capacity—absolute is required but hard to determine
- Appropriate Q_{st} equation model: $dP/dT = (S_1 - S_2) / (V_1 - V_2) = q_{st} / T(V_1 - V_2)$
- High-pressure effects—most common equation assumes ideal gas
- Q_{st} calculation protocol—most accurate way to calculate
- Temperature effects: understanding why Q_{st} estimates vary with temperature
- Temperature-dependence assumptions: this can affect Q_{st} results
- Heterogenous adsorption sites: how does this affect Q_{st} ?
- Best isotherm data fitting: which isotherms best capture the material physics?
- Determining equilibrium $K(T)$ accurately is needed for van't Hoff analysis
- Validity of van't Hoff: does it accurately apply to sorption processes?

LBNL

We have demonstrated frameworks with π -basic metals (Cu^I-MFU-4l and V^{II}-MOF) exhibit high adsorption enthalpy, which can be optimal for the room-temperature hydrogen storage. We will investigate to what degree the adsorption enthalpy of these frameworks can be tuned. Smaller pore analogues of Cu^I-MFU-4l and V^{II}-MOF will also be synthesized to increase volumetric hydrogen uptake capacities. During the evaluation of thermodynamic parameters of these materials, a very large temperature dependence of ΔH° and ΔS° upon H₂ adsorption has been observed in these frameworks by *in situ* DRIFTS measurements. The finding implies that thermodynamic parameters obtained at low temperatures may not describe behavior under conditions stipulated by DOE's ultimate storage targets. With *in situ* DRIFTS analysis we will "re-establish" some of the key parameters and physiochemical properties necessary for materials at the higher temperatures. Another approach to increase volumetric storage capacities is developing frameworks with low-coordinate metal sites. We have prepared a series of metalated frameworks; however, optimization for metalation and activation remains unsolved. We will continue metalation of frameworks with functionalized linkers to access low-coordinate metal sites. Thermodynamic properties of framework materials will be compared to the values predicted by computation. To this end, continuous efforts will be devoted to the development of a benchmark database, tailored for hydrogen binding with a variety of adsorption motifs, with the goal of providing inexpensive predictive analytics.

FY 2018 PUBLICATIONS/PRESENTATIONS

Publications

1. D. DeSantis, J.A. Mason, B.D. James, C. Houchins, J.R. Long, and M. Veenstra, “Techno-Economic Analysis of Metal–Organic Frameworks for Hydrogen and Natural Gas Storage,” *Energy Fuels* 31 (2017): 2024–2032.
2. E. Tsvion, S.P. Veccham, and M. Head-Gordon, “High Temperature Hydrogen Storage of Multiple molecules: Theoretical Insights from Metalated Catechols,” *ChemPhysChem* 18 (2017): 184–188.
3. E. Tsvion and M. Head-Gordon, “Methane Storage: Molecular Mechanisms Underlying Room-Temperature Adsorption in $Zn_4O(BDC)_3$ (MOF-5),” *J. Phys. Chem. C* 121 (2017): 12091–12100.
4. M.D. Allendorf, Z. Hulvey, T. Gennett, A. Ahmed, T. Autrey, J. Camp, E.S. Cho, H. Furukawa, M. Haranczyk, M. Head-Gordon, S. Jeong, A. Karkamkar, D. Liu, J.R. Long, K.R. Meihaus, I. Nayyar, R. Nazarov, D.J. Siegel, V. Stavila, J.J. Urban, S.P. Veccham, and B.C. Wood, “An Assessment of Strategies for the Development of Solid-State Adsorbents for Vehicular Hydrogen Storage,” *Energy Environ. Sci.* 11 (2018): 2784–2812.
5. M.T. Kapelewski, T. Runčevski, J.D. Tarver, H.Z.H. Jiang, A. Ayala, T. Gennett, S.A. FitzGerald, C.M. Brown, and J.R. Long, “Evaluating Metal–Organic Frameworks for High-Pressure H_2 Storage: Record High Volumetric Capacity in $Ni_2(m-dobdc)$,” *Chem. Mater.* In press.
6. H. Furukawa, “Synthesis and Characterization of Metal–Organic Frameworks,” in *Gas Adsorption in Metal-Organic Frameworks: Fundamentals and Applications*. (CRC Press, 2018). ISBN: 9780429469770 (ebook).
7. Mirjana Dimitrievska, Patrick Shea, Kyoung Kweon, Marnik Bercx, Joel B. Varley, Wan Si Tang, Alexander V. Skripov, Terrence J. Udovic, Vitalie Stavila, and Brandon C. Wood, “The Effects of Carbon and Anion Reorientational Dynamics in $LiCB_{11}H_{12}$ and $NaCB_{11}H_{12}$ Superionic Conductors,” *Adv. Energy Mater.* 8, no. 15 (2018): 1703422.
8. Wan Si Tang, Mirjana Dimitrievska, Vitalie Stavila, Wei Zhou, Hui Wu, A. Alec Talin, and Terrence J. Udovic, “Order-Disorder Transitions and Superionic Conductivity in the Sodium Nido-Undeca(car)borates,” *Chem. Mat.* 29, no. 24 (2017): 10496–10509.
9. Mirjana Dimitrievska, Vitalie Stavila, Alexei V. Soloninin, Roman V. Skoryunov, Olga A. Babanova, Hui Wu, Wei Zhou, Wan Si Tang, Antonio Faraone, Jacob D. Tarver, Benjamin A. Trump, Alexander V. Skripov, Terrence J. Udovic, “Nature of Decahydro-closo-decaborate Anion Reorientations in an Ordered Alkali-Metal Salt: $Rb_2B_{10}H_{10}$,” *J. Phys. Chem. C* 122, no. 27 (2018): 15198–15207.
10. Mirjana Dimitrievska, Jean-Noël Chotard, Raphaël Janot, Antonio Faraone, Wan Si Tang, Alexander V. Skripov, and Terrence J. Udovic, “Tracking the Progression of Anion Reorientational Behavior between α -phase and β -phase Alkali-Metal Silanides by Quasielastic Neutron Scattering,” *J. Phys. Chem. C* 122, no. 42 (2018): 23985–23997.
11. Marina Chong, Tom Autrey, and Craig Jensen, “Lewis Base Complexes of Magnesium Borohydride: Enhanced Kinetics and Product Selectivity upon Hydrogen Release,” *Inorganics* (2017), DOI:10.3390/inorganics5040089. Invited Special Issue: Functional Materials Based on Metal Hydrides, Inorganic Solid-State Chemistry.
12. Karsten Müller, Kriston Brooks, and Tom Autrey, “Hydrogen Storage in Formic Acid: A Comparison of Process Options,” *Energy and Fuels* (2017), DOI:10.1021/acs.energyfuels.7b02997.
13. Qi-Long Zhu, Fu-Zhan Song, Qiu-Ju Wang, Nobuko Tsumori, Yuichiro Himeda, Tom Autrey, and Qiang Xu, “Solvent-Switched In Situ Confinement Approach for Immobilizing Highly-Active Ultrafine Palladium Nanoparticles: Boosting Catalytic Hydrogen Evolution,” *J. Materials Chemistry A* (2018), DOI:10.1039/c8ta01093e.

14. Karsten Müller, Kriston Brooks, and Tom Autrey, “Releasing Hydrogen at High Pressures from Ambient Condition Carriers: Aspects for the H₂ Delivery to Fueling Stations,” *Energy and Fuels* (2018), DOI:10.1021/acs.energyfuels.8b0172.

Presentations

1. R. Chakraborty and M. Head-Gordon, “Multiscale Simulations in Chemistry with the Lattice Boltzmann Method,” Voth group at the University of Chicago, IL, February 8, 2018.
2. H. Furukawa, M.T. Kapelewski, H.Z.H. Jiang, T. Runčevski, Y.-Y. Lin, B.R. Barnett, K. Hou, G. Thiele, and J.R. Long, “Hydrogen Storage in Metal–Organic Frameworks,” 255th ACS National Meeting & Exposition, New Orleans, LA, March 21, 2018.
3. H.Z.H. Jiang and J.R. Long, “*In Situ* Characterization of Adsorbates in Nanoporous Materials with IR Spectroscopy,” 255th ACS National Meeting & Exposition, New Orleans, LA, March 22, 2018.
4. R. Chakraborty and M. Head-Gordon, “Modeling Adsorption with the Lattice Boltzmann Method,” West-Coast Theoretical Chemistry Symposium, Stanford University, CA, March 28, 2018.
5. J.R. Long, “HySCORE: LBNL Technical Activities–Hydrogen Storage in Metal–Organic Frameworks,” DOE H₂ Tech Team Meeting, Denver, CO, April 18, 2018.
6. B.R. Barnett, H.Z.H. Jiang, and J.R. Long, “Augmenting Hydrogen Sorption Enthalpies via Pi-Backdonation: Thermodynamic Ramifications for Optimizing Adsorptive Hydrogen Storage,” Organometallic Chemistry Gordon Research Conference, Newport, RI, July 10, 2018.
7. Philip Parilla, “Hydrogen Sorbent Measurement Qualification and Characterization,” 2017 AMR, Washington, DC, June 2017.
8. Philip Parilla and Thomas Gennett, “Hydrogen Storage Characterization and Optimization Research Effort within HyMARC,” ACS Meeting, New Orleans, LA, March 2018.
9. Katherine Hurst, “Results from a Multi-Laboratory Comparison of Hydrogen Volumetric Capacity Measurements,” ACS Meeting, New Orleans, LA, March 2018.
10. Katherine Hurst, “Update on NREL’s Validation Efforts: Inter-Laboratory Comparison,” Hydrogen Storage Tech Team Meeting, NREL, Golden, CO, April 2018.
11. Philip Parilla, “Update on NREL’s Characterization Efforts,” Hydrogen Storage Tech Team Meeting, NREL, Golden, CO, April 2018.
12. Thomas Gennett, “Update of Hydrogen Storage Initiatives,” McMinnville, Oregon, August 2017.
13. Thomas Gennett, “HySCORE Capabilities,” DOE FCTO Hydrogen Storage Kickoff Meeting, September 2017.
14. Thomas Gennett, “HySCORE Efforts and Capabilities,” HyMARC Consolidation Meeting, November 2017.
15. Katherine Hurst, Thomas Gennett, and Phil Parilla, Hydrogen Storage Tech Team Meeting, Detroit MI, September 2017.
16. Thomas Gennett, “Update on HySCORE Materials Efforts,” Hydrogen Storage Tech Team Meeting, NREL, Golden, CO, April 2018.
17. Thomas Gennett, “HySCORE: NREL Technical Activities,” 2017 AMR, Washington, DC, June 2017.
18. Thomas Gennett, “HySCORE: NREL Technical Activities,” H2@Scale Workshop, September 2017.
19. Thomas Gennett, “HySCORE,” ECS National Meeting, May 2017.
20. K. Hurst, S. Christensen, P. Parilla, and T. Gennett, “Modification of Borohydride Materials for Hydrogen Storage by ALD,” ALD 2017.

21. M. Dimitrievska, “Neutron Scattering Studies of Hydrogenous Materials for Next-Generation Energy Storage,” ACS National Meeting & Exposition, New Orleans, LA, 2018.
22. M. Dimitrievska, “Role of Solvent Adducts in Hydrogen Dynamics of Metal Borohydrides: Neutron-Scattering Characterization,” ACS National Meeting & Exposition, New Orleans, LA, 2018.
23. M. Dimitrievska, “Carbon Incorporation and Anion Dynamics as Synergistic Drivers for Ultrafast Diffusion in Superionic LiCB₁₁H₁₂ and NaCB₁₁H₁₂,” MRS Spring meeting, Phoenix, AZ, 2018.
24. M. Dimitrievska, “Neutron backscattering studies of hydrogenous materials for next-generation energy storage,” National Science Foundation Site Visit Review of Center for High Resolution Neutron Scattering (CHRNS), Washington, DC, 2018.
25. M. Dimitrievska, “Role of Solvent Adducts in Hydrogen Dynamics of Metal Borohydrides—Neutron-Scattering Characterization,” American Conference on Neutron Scattering, College Park, MD, June 2018.
26. T. Autrey, Boron Chemistry in the Americas (BORAM XVI), Boston College, June 26–30, 2018.
27. T. Autrey, Integration of Sustainable Energy Conference, Nuremberg, Germany, July 17–18, 2018.
28. T. Autrey, Department Seminar, Max Planck Institute, Stuttgart, July 20, 2018.
29. T. Autrey, Department Seminar, Montana State University, Oct 12, 2018.
30. T. Autrey, International Symposium on Metal-Hydrogen Systems, Guangzhou, China, October 2018.

REFERENCES

1. K. Hurst, T. Gennett, S. Shulda, and P. Parilla, “Results from a Multi-Laboratory Comparison of Hydrogen Volumetric Capacity Measurements,” in preparation 2018.
2. K.E. Hurst, P.A. Parilla, K.J. O'Neill, and T. Gennett, “An International Multi-Laboratory Investigation of Carbon-Based Hydrogen Sorbent Materials,” *Appl. Phys. A: Mater. Sci. Process.* 122, no. 1 (2016): 1–9.
3. S. Barbara, M. Ulrich, T. Natalia, S. Markus, F. Gérard, and H. Michael, “Heat of Adsorption for Hydrogen in Microporous High-Surface-Area Materials,” *ChemPhysChem* 9, no. 15 (2008): 2181–2184.
4. K.J. Gross, K.R. Carrington, S. Barcelo, A. Karkamkar, J. Purewal, S. Ma, H.-C. Zhou, P. Dantzer, K. Ott, T. Burrell, T. Semeslberger, Y. Pivak, B. Dam, D. Chandra, and P. Parilla, *Recommended Best Practices for the Characterization of Storage Properties of Hydrogen Storage Materials*, V3.34 (H2 Technology Consulting LLC, 2012), http://www1.eere.energy.gov/hydrogenandfuelcells/pdfs/best_practices_hydrogen_storage.pdf.
5. D.P. Broom, *Hydrogen Storage Materials: The Characterisation of Their Storage Properties*, (Springer: London; New York, 2011).
6. K.S.W. Sing, F. Rouquerol, and J. Rouquerol, “5-Classical Interpretation of Physisorption Isotherms at the Gas–Solid Interface,” In *Adsorption by Powders and Porous Solids* (Second Edition), Rouquerol, F.; Rouquerol, J.; Sing, K.S.W.; Llewellyn, P.; Maurin, G., Eds. (Academic Press: Oxford, 2014): 159–189.
7. F.O. Mertens, “Determination of Absolute Adsorption in Highly Ordered Porous Media,” *Surface Science* 603, no. 10 (2009): 1979–1984.
8. C.O. Areán, S. Chavan, C.P. Cabello, E. Garrone, and G.T. Palomino, “Thermodynamics of Hydrogen Adsorption on Metal–Organic Frameworks,” *ChemPhysChem* 11 (2010): 3237–3242.
9. D. Denysenko, M. Grzywa, J. Jelic, K. Reuter, and D. Volkmer, *Angew. Chem. Int. Ed.* 53 (2014): 5832–5836.
10. E. Garrone, B. Bonelli, and C. Otero Areán, “Enthalpy–Entropy Correlation for Hydrogen Adsorption on Zeolites,” *Chem. Phys. Lett.* 456 (2008): 68–70.